Semibatch Reaction Crystallization of Benzoic Acid

Bengt L. Åslund and Åke C. Rasmuson
Dept. of Chemical Engineering, The Royal Institute of Technology, S - 100 44 Stockholm, Sweden

An experimental study of a semibatch reaction crystallization is presented. Dilute hydrochloric acid is fed to a stirred solution of sodium benzoate to crystallize benzoic acid. The weight mean size of the product crystals increases with increasing stirring rate, reaches a maximum, and then decreases again. Larger crystals may be produced if the reactant feed point is positioned close to the outlet stream of the impeller. At equal power input the influence of stirrer type is negligible. Decreasing reactant concentrations or feed rate increases the crystal size significantly. Experimental results are explained qualitatively focusing on nucleation and growth conditions and on feed point mixing. The feed point micromixing brings reactants together to generate supersaturation and allow for nucleation. Continued mixing, however, may partially dilute supersaturation before nucleation takes place or may restrict nuclei growth, thus promoting more efficient Ostwald ripening in the bulk. This may result in high bulk supersaturations which in turn hampers the dilution effects.

Introduction

In reaction crystallization, a solution of one reactant often is mixed with a solution of the other, and the crystallizing substance is formed by a chemical reaction in concentrations exceeding the solubility. Frequently, the reaction is fast or very fast, and the mixing conditions influence the product size distribution significantly. In a batch experiment, the entire volumes of the two reactant solutions are mixed instantaneously in a stirred vessel. In a continuous process, both solutions are fed to the vessel, and there is a continuous or semicontinuous withdrawal of product suspension. In a semibatch process, there is no outlet. An often used technique is to feed a solution of one of the reactants to a stirred solution of the other.

Table 1 shows previous research results on the influence of different process parameters on the product in solution reaction crystallization. An arrow pointing upward denotes an increase and downward denotes a decrease in product mean size as the process parameter in question increases. These results are sometimes contradictory. In semibatch experiments, larger crystals of potash alum are obtained, as compared to a batch process (Mullin et al., 1982). Tosun (1988) found that feeding the two reactant solutions simultaneously to the stirred tank (semibatch) results in larger crystals than feeding one reactant to a stirred solution of the other; however, the results are not entirely comparable. By feeding reactants apart in the double-feed semibatch crystallization of barium sulfate, larger crystals are produced than when the feed points are close (Tosun, 1988; Kuboi et al., 1986). O'Hern and Rush (1963) found continuous precipitation to produce significantly larger particles of barium sulfate than batch processing and mixing in "rapid mixers." Particularly, at higher concentrations the continuous stirred vessel produces much larger particles. These results are in accordance with those of Tosun (1988), a simple side-T mixer produced much smaller crystals than stirred vessel precipitation. The side-T results reveal a decreasing size at increasing Reynolds number.

O'Hern and Rush (1963) mentioned that the maximum nucleation rate occurs at maximum mean ionic molality and that in a stirred vessel the flow pattern shows a great deal of recirculation and dilution of the entering reagents. Gutoff et al. (1978) discussed a nucleation zone around the feed entrance from which nucleous are conveyed into a bulk volume for Ostwald ripening. The influence of agitation and feed conditions on the size of the feed zone is used to explain different product sizes. Tosun (1988) applied a similar concept and suggested that a nucleation zone delivers nucleous and supersa-

Correspondence concerning this article should be addressed to Å C. Rasmuson.

Table 1. Influence of Operating Parameters on Crystal Size

Effect	Process*	Substance	Reference
Increased Stirring Rate (N)			
↓	Batch	Barium Sulfate	Pohorecki and Baldyga (1983)
	Semibatch (*S*)	Barium Sulfate	Tosun (1988)
		Silver Bromide	Gutoff et al. (1978)
↑	Semibatch (*D*)	Barium Sulfate	Tosun (1988)
↓		Silver Chloride	Stavek et al. (1988)
↑	Continuous	Barium Sulfate	Pohorecki and Baldyga (1985)
↑		Barium Sulfate	Fitchett and Tarbell (1990)
—		Salicylic Acid	Franck et al. (1988)
Increased Feed Point Mixing at Constant Stirring Rate			
↓ (Low N)	Semibatch (*S*)	Barium Sulfate	Tosun (1988)
↑ (High N)		Barium Sulfate	Tosun (1988)
↓	Semibatch (*D*)	Barium Sulfate	Tosun (1988)
↑			
Increased Feed Rate			
↓	Semibatch (*S*)	Cadmium Sulfide	Ramsden (1985)
↓		Silver Bromide	Gutoff et al. (1978)
—		Potash Alum	Mullin et al. (1982)
Increased Reactant Concentrations			
↓	Batch	Barium Sulfate	Pohorecki and Baldyga (1983)
↓		Nickel Ammonium Sulfate	Mullin and Osman (1973)
↓		Potash Alum	Mullin et al. (1982)
↓		Salicylic Acid	Franck et al. (1988)
↑		Barium Sulfate	Gunn and Murthy (1972)
↑		Magnesium Hydroxide	Gunn and Murthy (1972)
↓	Continuous	Barium Sulfate	Pohorecki and Baldyga (1985)
—		Barium Sulfate	O'Hern and Rush (1963)
—		Salicylic Acid	Franck et al. (1988)
Increased Residence Time			
↑	Continuous	Sulfamic Acid	Toyokura et al. (1979)
↑		Silver Bromide	Wey et al. (1980)
↑		Barium Sulfate	Pohorecki and Baldyga (1985)
↑		Salicylic Acid	Franck et al. (1988)

*S = single feed of reactants; D = double feed of reactants; N = stirring rate

turation to a growth zone. Mohanty et al. (1988), in their study on reaction crystallization in a mixing-T process, found about 10 times higher number of barium sulfate crystals from a long T than a short T, and concluded that this is mainly the result of fragmentation or secondary nucleation, not of continued primary nucleation. A significant influence of mixing on primary nucleation was seen only at supersaturation ratios ($S = c/c_s$) above 3,000. Fitchett and Tarbell (1990) used an MSMPR crystallizer and found the nucleation rate to decrease with increased mixing. This was explained as being the result of reduced supersaturation due to an increased growth rate. Tavare and Garside (1990) modeled a semibatch process, in which both reactants are fed in separate feed streams and crystallizer is assumed perfectly mixed and Ostwald ripening is included in the model. The results show that reactant addition rate profiles may be used to exercise product control.

Research on reaction crystallization shows contradictions concerning the influence of process variables like stirring rate and reactant concentrations on the product crystal size and the understanding of mechanisms is inconclusive. This article presents a comprehensive set of well-documented experimental results on the influence of process variables on the product size distribution in a semibatch reaction crystallization process. The mechanisms controlling the process, particularly mixing effects and crystal nucleation, are analyzed and the experimental results are qualitatively explained.

Experimental Studies

Benzoic acid is crystallized by adding dilute hydrochloric acid to a stirred aqueous solution of sodium benzoate, and in some cases by adding sodium benzoate to hydrochloric acid. The influence of impeller rotational speed, feed point position, impeller type, feed rate and reactant concentrations are explored. Benzoic acid is low-soluble, but not sparingly soluble in water. At 30°C the solubility in pure water is 0.42 g/100 g H_2O, and at 18°C the corresponding value is 0.27 (Kirk-Othmer, 1979). In 0.35 mol/L sodium benzoate solution and in 0.28 mol/L sodium chloride solution (bulk concentration at the end in the majority of the experiments), the solubilities at 18°C are 0.30 and 0.25 g/100 g H_2O, respectively (Larsson, 1930). At higher sodium chloride concentration and the same temperature, the solubility becomes lower. For 0.35 mol/L and 1.4 mol/L, it becomes 0.24 and 0.16 g/100 g H_2O, respectively. Benzoic acid crystallizes as needles or as leaflets (Kirk-Othmer, 1979).

Apparatus

The crystallizer is a 1-L glass tank reactor equipped with four baffles of stainless steel and of dimensions in Figure 1. The flat-bottom tank is immersed in a thermostatic bath to maintain a temperature of 30°C throughout the experiments. The liquid level in the tank is 96 mm in most cases at the

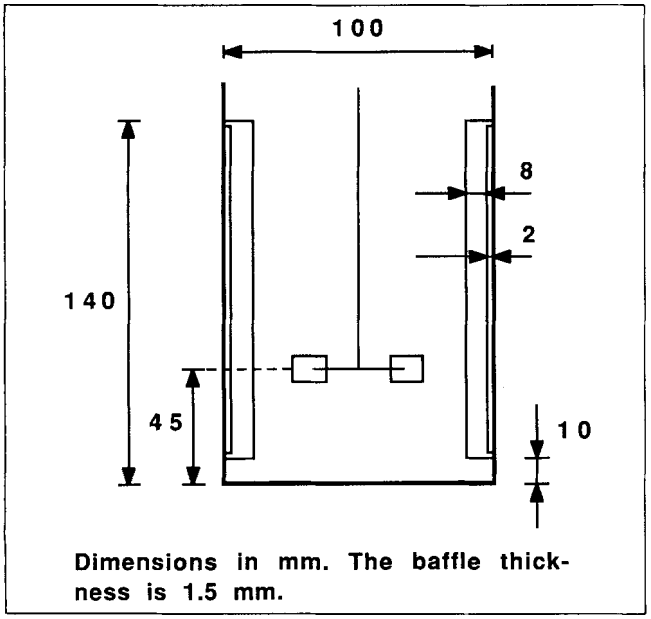

Figure 1. Crystallizer geometry.

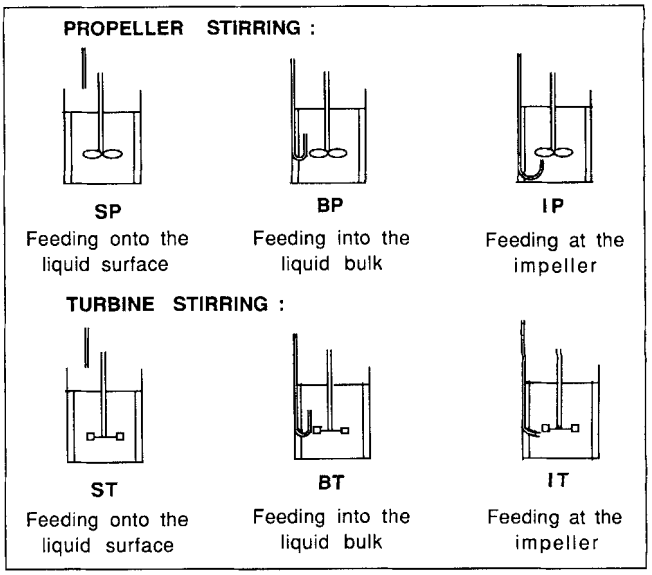

Figure 3. Reactant feed point position and notation.

beginning of the experiment and 118 mm at the end when all the acid has been added. In experiments where the effect of the reactant concentrations are examined, the liquid level ends in the range 100 to 150 mm. A six-blade disc turbine (T) (Rushton type) of stainless steel and a three-blade marine-type propeller (P) of stainless steel are used at rotational speeds from 200 to 1,600 RPM. The impellers are shown in Figure 2.

A two-piston pump (Desaga 2000) is used for feeding. The pumping rate is controlled by a small computer, and a function generator feeds stepping pulses to the pump. Each step of a piston delivers 4 μL, and the maximum rate is 165 steps/s. The pumping rate may be changed every third second by the computer program. Pumping and filling instructions are given in such a way that no interruption of the reactant flow occurs during the experiment. The feed point is located on the liquid surface (S), and inside the liquid bulk (B) or the exit stream close to the impeller (I), Figure 3. Feeding into liquid bulk is done cocurrently to the flow direction, while addition at the impeller is done countercurrently to the flow. When feeding is on the surface, the position of the pipe outlet is half a tank radius from the impeller axis and about 50 mm above the solution surface. When feeding gets into the bulk, the pipe outlet is located 20 mm from the wall, half-way between two baffles and 20 mm above the impeller blade. For the turbine, feeding close to the impeller is done just below the turbine blade and approximately 5 mm from the blade in the horizontal direction. In the case of the propeller, feeding close to the impeller is done half a propeller blade horizontally away from the rotation axis and 5 to 10 mm below the propeller. The feed pipe is made of glass and the internal diameter is 1.5 mm.

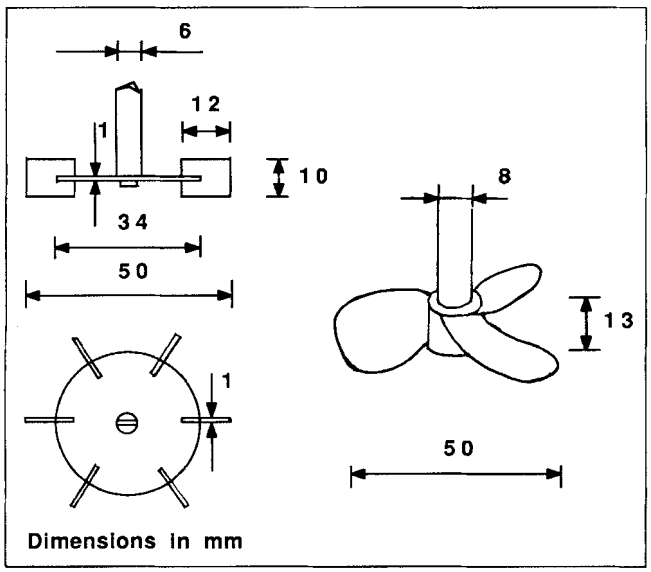

Figure 2. Stirrers.

Procedures

In all experiments, by the end, stoichiometric amounts have been mixed. The initial benzoate solution is saturated with benzoic acid and contains a corresponding stoichiometric amount of sodium chloride. The sodium benzoate solution and distilled water used for dilution of hydrochloric acid are filtered through a 0.22-μm membrane filter before the experiment. In the experiments on the influence of stirring rate, feed point position and stirrer type, 173 mL of 1.4 mol/L hydrochloric acid is added during 90 minutes (1.9 mL/min) to 688 mL of 0.35 mol/L sodium benzoate solution. The influence of feed rate (0.3 to 12 mL/min) is studied for some hydrodynamic conditions and concentrations. In all cases, however, acid is fed to 688 mL of 0.35 mol/L sodium benzoate solution. Ultimate stoichiometry is always attained, and the total feed time thus ranges from 36 to 360 minutes. The influence of acid concentration has been examined by feeding solution of low (0.56 mol/L) and high (3.51 mol/L) concentration of hydrochloric acid to solution of standard (0.35 mol/L) concentration of benzoate at IT 400 and for two different acid molar feed rates. Further experiments on the influence of concentrations

Table 2. Experimental Reproducibility

Feed Point	Stirrer Type	Stirrer Speed (RPM)	No. of Exp.	Mean of Wt. Mean Size (μm)	Std. Dev. of Wt. Mean Size (μm)
Surface	Propeller	800	2	29.4	1.1
		1,600	2	28.5	2.8
	Turbine	800	2	30.6	1.4
Bulk	Propeller	200	2	17.8	0.3
		1,600	4	27.8	1.5
	Turbine	200	2	23.5	1.4
		800	2	28.4	1.9
		1,600	2	25.3	4.5
Impeller	Turbine	200	3	30.0	0.3
		800	2	27.2	0.1
		1,600	2	23.9	0.9

comprise feeding different hydrochloric acid solutions to low (0.14 mol/L) and high (0.88 mol/L) initial concentrations of sodium benzoate solution (688 mL) and a few experiments on feeding benzoate solution to a stirred solution of hydrochloric acid.

At the very beginning of a moderately stirred experiment, a cloudy volume or plume containing nuclei or tiny crystals of benzoic acid is seen at the feed point. The bulk liquid remains transparent, and no particles are seen for about 3 to 5 minutes. The turbidity of the bulk increases gradually with time. If the mixing intensity is high, air bubbles are continuously drawn into the solution making the liquid opaque from the start. The particulate product may be described as rather weak flocks or aggregates of benzoic acid crystals. By addition of a surface-active agent followed by ultrasonic treatment an almost complete disintegration into free single crystals is achieved. The crystals are thin, rectangular plates. Aggregated they form chains of variable lengths.

An electrosensing zone instrument (ELZONE 180 X Y) is used to measure the product particle size distribution. At the end of the experiment, two samples, 20 mL each, are taken from the center of the stirred reactor. At low experimental rotational speed, the stirring rate is increased before sampling to get a well-mixed suspension. One sample is used for determination of the crystal size distribution. Two to three drops of surfactant are added and then it is stored in a thermostatic bath (30°C) for approximately 20 minutes (which does not affect the size distribution of individual crystals). Just before analysis the sample is inserted three times into an ultrasonic bath for 5 seconds each time. One to three drops are mixed into 130-mL electrolyte, and the size distribution is determined. The electrolyte solution is saturated by benzoic acid and is filtered (0.22 μm) prior to use. For crystal size determination, three drops of surfactant have been added to the electrolyte. The measuring cup is a jacketed glass vessel thermostated to 30°C. The other sample is analyzed directly to determine the product particle or aggregate size distribution.

Results are presented in terms of relative mass density distributions. The relative mass density is defined as the crystal mass in a size interval divided by the total mass of crystals and divided by the width of the size interval (ΔL). The particle size is defined as equivalent spherical diameter, as obtained from the particle volume measured by the particle analyzer. The weight mean size (L_{43}) and the width of the size distribution (SD), calculated as a standard deviation around the weight mean size, are defined as:

$$L_{43}=\frac{\Sigma N_i L_i^4}{\Sigma N_i L_i^3} \qquad SD=\sqrt{\frac{\Sigma(L_i-L_{43})^2 N_i L_i^3}{\Sigma N_i L_i^3}}$$

N_i is the number of particles in a size interval, and L_i is the geometric mean size of that interval.

Results

Aggregate weight mean size ranges from 74 to 182 μm,and the distribution width from 21 to 63 μm. The aggregate size distributions do not correlate with changes in the process variables. The aggregates are easily broken, and the stirring conditions in the particle size analysis are important. Only the influence of process parameters on the product crystal size distribution is evaluated here as obtained by disintegration of product aggregates. Results on the total size distributions are presented by Åslund and Rasmuson (1990), and complete results are given by Åslund (1989). The crystal weight size distributions are unimodal and somewhat skewed to larger sizes, like a gamma distribution. In an introductory study (Åslund and Rasmuson, 1989), a good reproducibility of crystal size distributions and weight mean sizes are reported. This conclusion is supported by the results in Table 2 showing the standard deviation of the weight mean size of the product crystals. The reproducibility is somewhat lower at the highest stirring rate which could be related to significant amounts of air being drawn into the suspension at these conditions.

The influence of stirring rate on the product weight mean size is shown in Figure 4. The size of the product crystals increases with increasing stirring rate, reaches a maximum, and then decreases. The optimum stirring rate for production of large crystals depends on feed point position and stirrer type. At propeller stirring the decrease at high stirring rates is less pronounced. Feeding close to the turbine produces large particles already at the lowest stirring rate, and a decrease in size is seen already at 800 RPM. The crystals produced at 1,600 RPM are even smaller than those formed at 200 RPM.

The influence of feed point position on the weight mean size is shown in Figure 5. At low stirring rates, significantly larger crystals are obtained if the reactant is fed close to the stirrer.

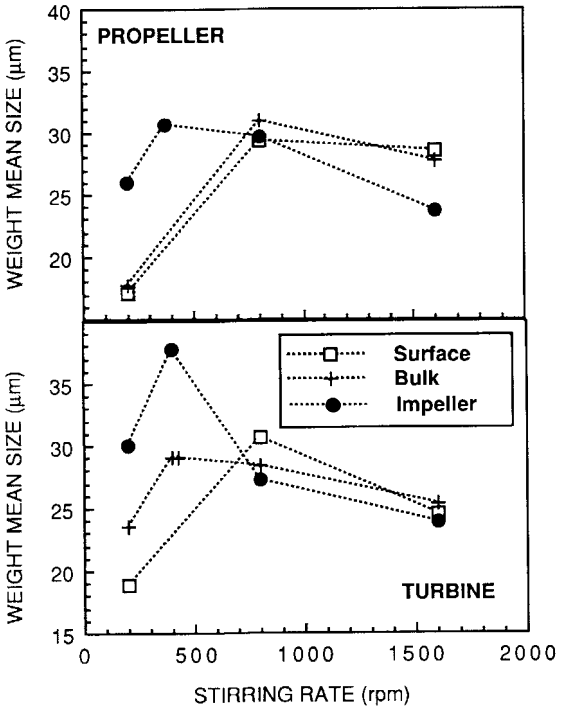

Figure 4. Influence of stirring rate on crystal weight mean size.

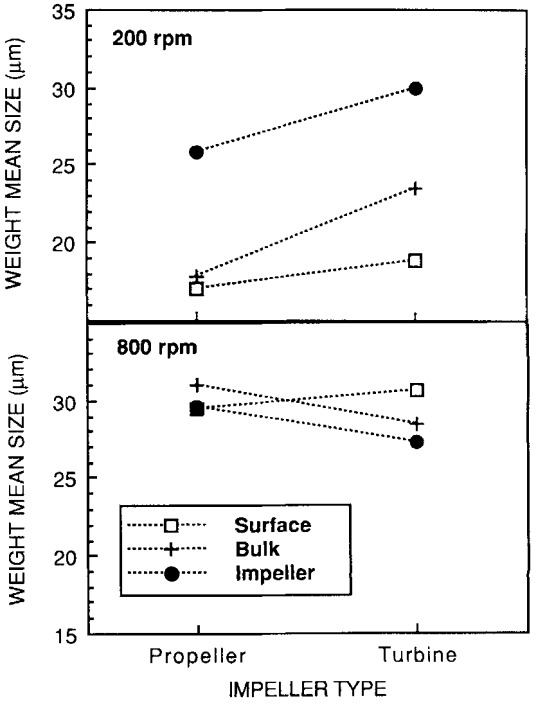

Figure 6. Influence of impeller type on crystal weight mean size at equal stirring rates.

The smallest crystals result from feeding onto the liquid surface. At 800 RPM, the influence of the feed point position is much weaker and almost within the experimental uncertainty. At 1,600 RPM, the best position for the propeller is onto the surface and the worst close to the stirrer.

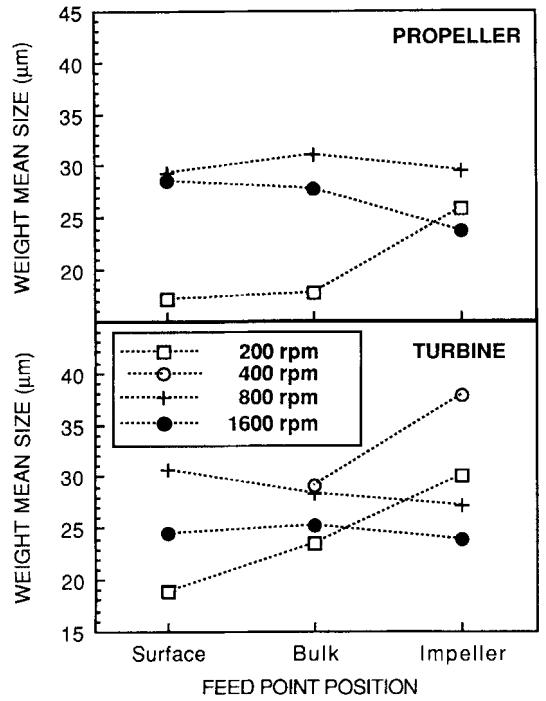

Figure 5. Influence of feed point position on crystal weight mean size.

The influence of the stirrer type is shown in Figure 6. At 200 RPM, regardless of feed point position, larger crystals are obtained if the turbine is used instead of the propeller at equal stirring rates. At higher stirring rates, the influence of stirrer type tends to be reversed. At equal stirring rates, the power input of the turbine is approximately 6.6 times the input of the propeller (Oldshue, 1983). Since the power input is proportional to the stirring rate raised to power 3, the corresponding relation between stirring rates at equal power input is 1.9. The comparisons in Table 3 show that regardless of feed point position and stirring rate, the influence of stirrer type at equal power input is negligible. These comparisons cover a 64-fold range of mean power inputs, where the 426/800 RPM data corresponds to approximately ten times the power input of the 200/375 RPM experiments. One single exception to the conclusion results from the high value of IT 400 (L_{43} = 37.8 μm) almost comparable to the mean power input of IP 800 (L_{43} = 29.6 μm).

Table 3. Influence of Stirrer Type at Equal Power Input

Feed Point	Stirrer Type	Stirrer Speed (RPM)	Wt. Mean Size (μm)
Surface	Propeller	1,600	28.5
	Turbine	800	30.6
Bulk	Propeller	800	31.0
	Turbine	426	29.0
	Propeller	1,600	27.8
	Turbine	800	28.4
Impeller	Propeller	375	30.6
	Turbine	200	30.0
	Propeller	1,600	23.7
	Turbine	800	27.2

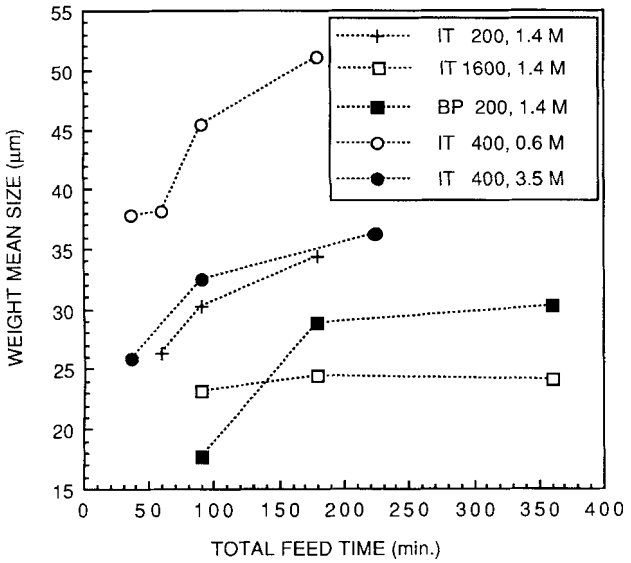

Figure 7. Influence of total feed time (reactant feed rate) on crystal weight mean size.

The influence of the reactant feed rate, that is, the total feed time, on the product crystal weight mean size is shown in Figure 7 for different hydrodynamic conditions and acid concentrations. Larger crystals are produced when the total feed time increases, but the influence gradually disappears. At 1,600 RPM, the crystal size distribution is unaffected by the feed rate. In a few experiments, the feed rate is gradually increased or decreased according to a second-order dependence of time. No strong influence is seen and, the results on the influence of feed rate profile is inconclusive. Experiments with pulsed feeding of evenly distributed feeding periods resulted in smaller product crystals than continuous feeding during the same total time.

The influence of reactant concentrations is evaluated using turbine stirring at 400 RPM and feeding close to the impeller. By decreasing the hydrochloric acid concentration, the crystal weight mean size increases significantly as shown in Figure 8. The experiments comprise two total feed times corresponding to two different acid molar feed rates. The initial sodium benzoate concentration is 0.35 mol/L in all cases. To keep

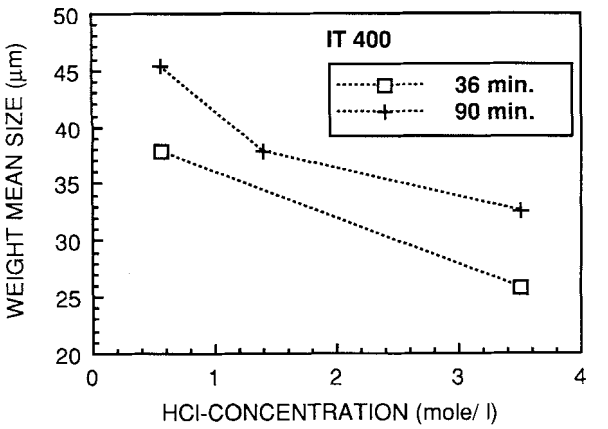

Figure 8. Influence of hydrochloric acid concentration on crystal weight mean size.

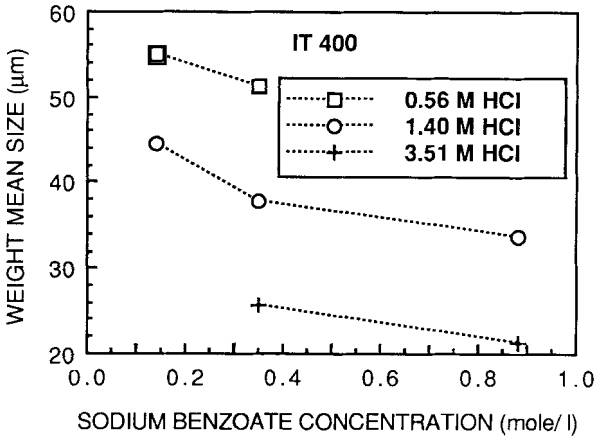

Figure 9. Influence of sodium benzoate concentration on crystal weight mean size.

ultimate stoichiometry, the total volume fed is reduced (the volume flow rate is reduced), as the acid concentration is increased. In Figure 9, the influence of the sodium benzoate concentration on the weight mean size is shown. Along with an increase in benzoate concentration, the total time of acid feeding is increased at constant volume feed flow rate to meet stoichiometry. In each curve, the acid concentration, as well as the acid molar feed flow rate, is constant. A decrease in sodium benzoate concentration significantly increases the product crystal size.

Feeding hydrochloric acid into a solution of sodium benzoate at moderate stirring rates produces larger crystals than feeding sodium benzoate into hydrochloric acid, Figure 10. The 173-mL solution of the 1.4-mol reactant/L is fed into 688 mL of the 0.35 mol/L stirred reactant. Feeding is close to the turbine for 90 minutes. At higher stirring rates, the difference vanishes.

The width of the crystal size distribution depends on process variables. However, this dependence is related strongly to the weight mean size of the product crystals, as is shown in Figure 11. The figure presents all the results of various process conditions. An increase in weight mean size is accompanied by an increase in size distribution width. The width is approximately directly proportional to the mean size and the coefficient of variation becomes approximately 0.3. No other specific correlation to process variables has been recognized.

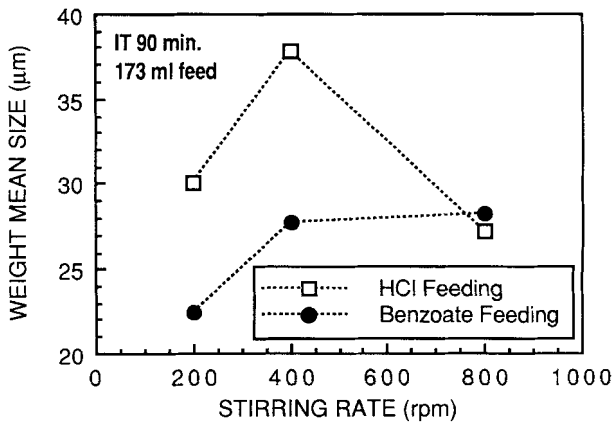

Figure 10. Influence of feed substance on crystal weight mean size.

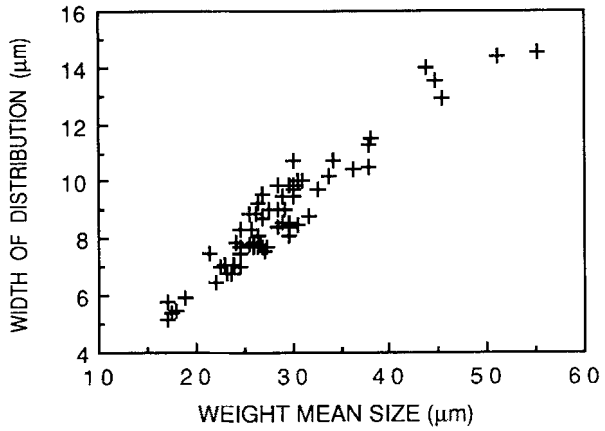

Figure 11. Crystal size distribution width as function of weight mean size.

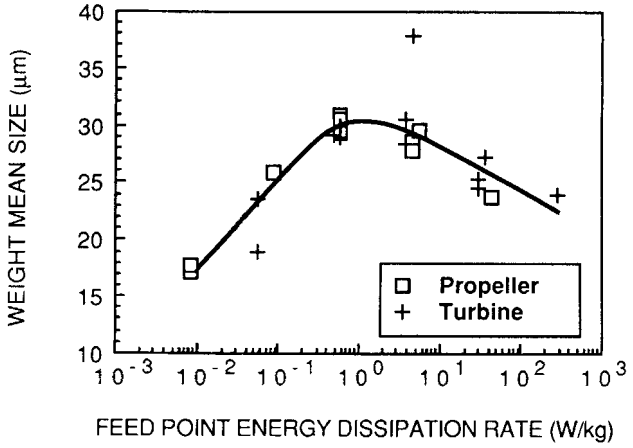

Figure 12. Weight mean size as function of feed point energy dissipation rate.

Evaluation

In a semibatch reaction crystallization, the hydrodynamics may significantly influence the size of product crystals. In the experiments, the product crystal weight mean size ranges from 17 μm to 37 μm depending on the stirring rate and the reactant feed point position. At increasing stirring rate, the weight mean size increases, attains a maximum and then decreases. At low stirring rates, the influence of the feed position is to produce larger crystals as the reactant is fed at locations of increased mixing intensity. Appropriate positioning of the feed is as equally important in producing large crystals as an increase in stirring rate; the latter, however, achieved by increased energy consumption and capital investment. At high overall mixing intensity, the influence of the feed point location becomes negligible. At low agitation, the turbine agitator produces larger crystals than the propeller at equal stirring rates, but the influence of the stirrer type at equal power input is negligible. Tosun (1988) studied crystallization of barium sulfate by feeding sodium sulfate into a stirred solution of barium chloride and found the crystal mean size to decrease to a minimum with increasing stirring rate. A further increase of the stirring rate resulted in increased mean size. Concerning the influence of the reactant feed point position, an increase in size was found with increasing feed point mixing intensity. For silver halide, an increase in size with increased agitation is reported for semibatch processes (Gutoff et al., 1978).

The mean power input per unit mass in the experiments is estimated (using graphs of Oldshue, 1983) to be 0.1 W/kg for 200-RPM turbine stirring and to 0.014 W/kg for 200-RPM propeller stirring. The mean power input is proportional to the stirring rate raised to 3. Accordingly, the ratio of the mean power input for 200, 800 and 1,600 RPM is 1 : 64 : 512. At equal stirring rate, the power input of the turbine is about 6.6 times the power input of the propeller. Okamoto et al. (1981) measured the distribution of the energy dissipation rate in stirred tanks and found the local dissipation rate to vary by a factor of 40. Roughly, the ratio of the local energy dissipation rate close to the surface, in the bulk, and close to the impeller is 1 : 1 : 10. We estimate the energy dissipation close to the stirrer to be six times the specific mean power input and in the bulk to be 0.6 the mean value. In Figure 12, the mean product size for all experiments concerning the influence of hydrodynamics (in all experiments the concentrations and feed rate are the same) is plotted vs. the estimated local energy dissipation rate at the feed point. At low stirring rates, an increased feed point energy dissipation rate increases the product size to a maximum. Increasing the energy dissipation rate further decreases the weight mean size. Data on the mean size vs. mean power input show the same features, but they are more scattered in the low dissipation range.

In crystallization, mixing often is kept low enough to only suspend the crystals from the bottom. An increased intensity promotes secondary nucleation, attrition and breakage more than the growth of crystals. Figure 13 shows the crystals obtained from the product through treatment by surfactant and ultrasonics. While the crystals are rather nicely shaped at 200 RPM, they become increasingly damaged as the rotational speed increases. At 1,600 RPM, corners and edges are rounded, and the crystals in general look damaged and rather irregular. Some of the crystals seem to be cracked, and inclusions of solution may be present. Rousseau et al., (1976) suggest that secondary nucleation depends on crystal size and might be negligible at 30 μm. As described earlier, however, the dominating particles in the crystallizer are aggregates much larger than 30 μm. At collisions with one another and with the equipment, not only the aggregates break, but the crystals in the aggregates may be damaged. Also, the mixing intensity at higher stirring rates in the experiments is higher than is usually the case in crystallization processes. Furthermore, the benzoic acid crystals in this study are rather thin plates, more easily broken than compact shapes. In conclusion, secondary nucleation, attrition and breakage may be active at high stirring rates and may contribute to the product size decrease at high mixing intensities. These mechanisms, however, do not in particular relate to feed point conditions and accordingly may not explain the 1,600-RPM curve of the upper diagram or the 800-RPM curve of the lower diagram of Figure 5. However, the lower mean size and the lack of dependence on feed point at 1,600-RPM impeller stirring are likely to result from these effects.

A reduced feed rate at low stirring rates results in larger crystals independent of hydrochloric acid concentration. As an example, the weight mean size ranges from 51 μm at 180-min to 38 μm at 36-min feed time, when hydrochloric acid of

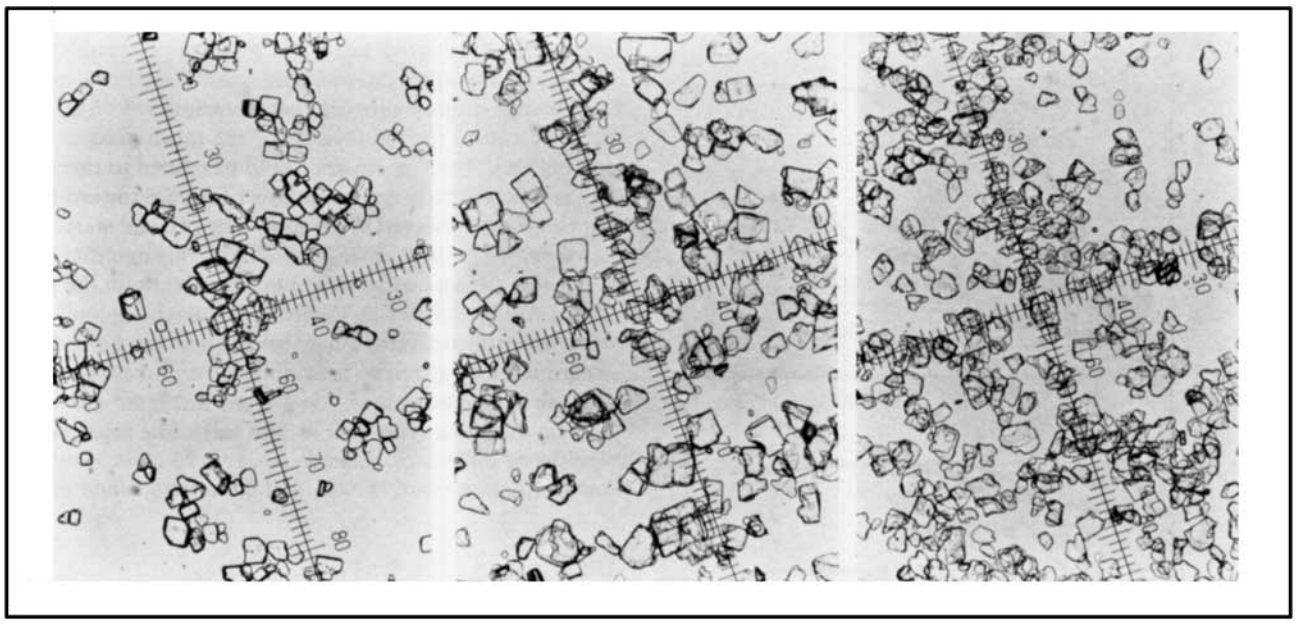

Figure 13. Product crystals obtained after aggregate disintegration.

From experiments applying turbine stirring and reactant feeding at the impeller. Stirring rates: 200, 800 and 1,600 RPM, respectively, from left to right.

low concentration is added. At high stirring rates, the crystal weight mean size is not influenced significantly by the reactant feed rate. This is in agreement with the results of Gutoff et al. (1978) for silver bromide. Significantly larger crystals are produced in this study by decreasing the reactant concentrations. In Figure 14, the weight mean size is plotted vs. the logarithm of the product of the initial reactant concentrations. For each curve the total feed time, added volume of hydrochloric acid, and ratio of the initial reactant concentrations are constant. In all cases, the product crystal weight mean size increases significantly as reactant concentrations decrease. A sixfold increase of both concentrations reduces the mean size from 55 μm to 21 μm. These results correspond to what's normally observed in other process configurations. In batchwise experiments, Franck et al. (1988) found that the product mean size of salicylic acid decreases with increased initial concentrations of the reactants. The same conclusions were drawn

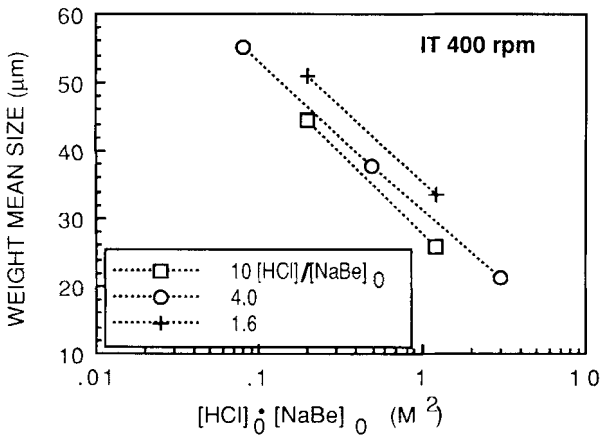

Figure 14. Weight mean size as function of the product of initial reactant concentrations.

by Pohorecki and Baldyga (1983) for crystallization of barium sulfate, Mullin and Osman (1973) for nickel ammonium sulfate, and Mullin et al. (1982) for potash alum.

In some cases, the suspension has been sampled during the experiment. In Figure 15, the total number of detectable crystals and the weight mean size as functions of elapsed time are plotted for four different experiments. The feed point energy dissipation rate ranges, over approximately four orders of magnitude, from BP 200 to IT 1600. Due to experimental uncertainties, the absolute numbers of crystals should be regarded as approximate. The change in total number of crystals reflects the net result of nucleation, ripening, abrasion and breakage, (agglomeration is not seen in these curves since they relate to disintegrated samples). In the BP 200 experiment, the net particle generation rate is rather constant during the first half of the experiment, but decreases significantly toward the end. In IT 200, the energy dissipation at the feed point is increased about 66 times. The net generation rate in this experiment is significantly lower during the first 30 minutes, resulting in larger mean sizes. At further increased mixing, BP 1600, the net particle generation rate early in the process is higher again and the mean size is accordingly lower. In IT 1600, the maximum mixing intensity is at hand in terms of bulk mixing, particularly in terms of feed point mixing. The particle generation rate early in the process is increased further and it is even higher than that in BP 200. Furthermore, there is a significant increase toward the end due perhaps to secondary nucleation, abrasion and breakage.

Figure 16 shows weight and population density distributions for the IT 200 and the IT 1600 experiments, whose evolution of the size distributions quite differs. At 200 RPM, the relative weight distribution is rather constant during the first 30 minutes of the process, but the population density increases over the whole size range. Toward the end, the weight mean size increases. At 1,600 RPM, there is an evolution of the weight distribution from start. The weight mean size is constant to-

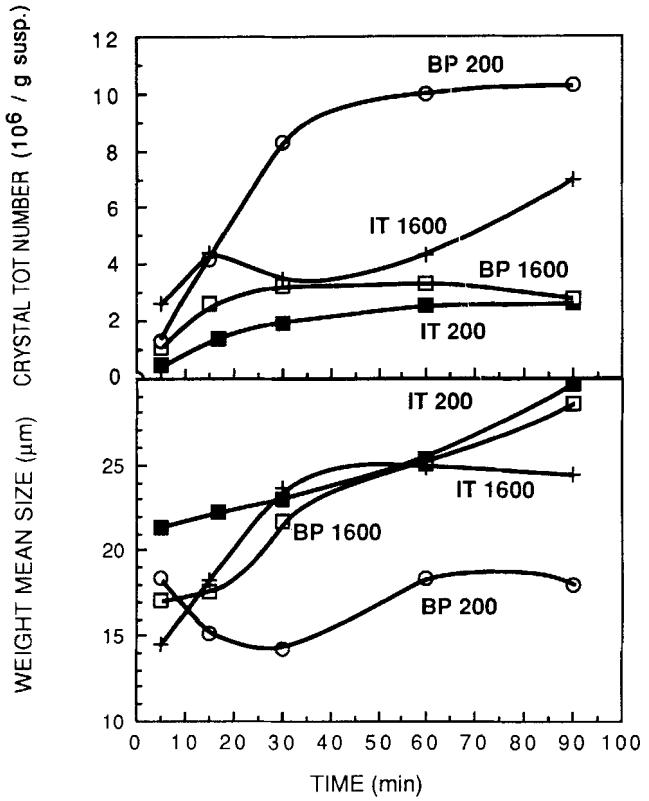

Figure 15. Total number of crystals and weight mean size as function of elapsed experimental time.

ward the end. The 1,600-RPM curves suggest that too many crystals are generated early and the largest crystals may be broken into smaller, intermediate sizes. Figures 15 and 16 do not unambiguously support that abrasion and breakage are the only causes for the reversal of the mean product size vs. stirring rate. These processes would be related to magma density and particularly cause a number increase toward the end, which is only observed in IT 1600. The reversal starts already at much lower mixing intensities. The mixing intensity strongly influences the rate of particle generation early in the process. This is further verified by Figure 17, in which the total number of particles at different times are plotted for eight different experiments at different feed point energy dissipation rates. At high dissipation rates, there is an increased particle production at the early as well as late stage, the latter seen as a significant difference between 60- and 90-minute values. At low dissipation rates, the 60- and 90-minute values coincide.

Discussion

The results presented suggest that the concentration levels at the feed point are of major importance. The higher the local concentrations, the smaller becomes the product particles. This indicates that local nucleation at the feed point controls the product size distribution. The results also suggest that increased local mixing reduces this nucleation, at least at moderate mixing intensities. The crystal growth rate may increase with increasing mean power input, if growth is volume diffusion controlled; this may have some importance in the process. An influence on the larger crystals in the bulk, however, do not

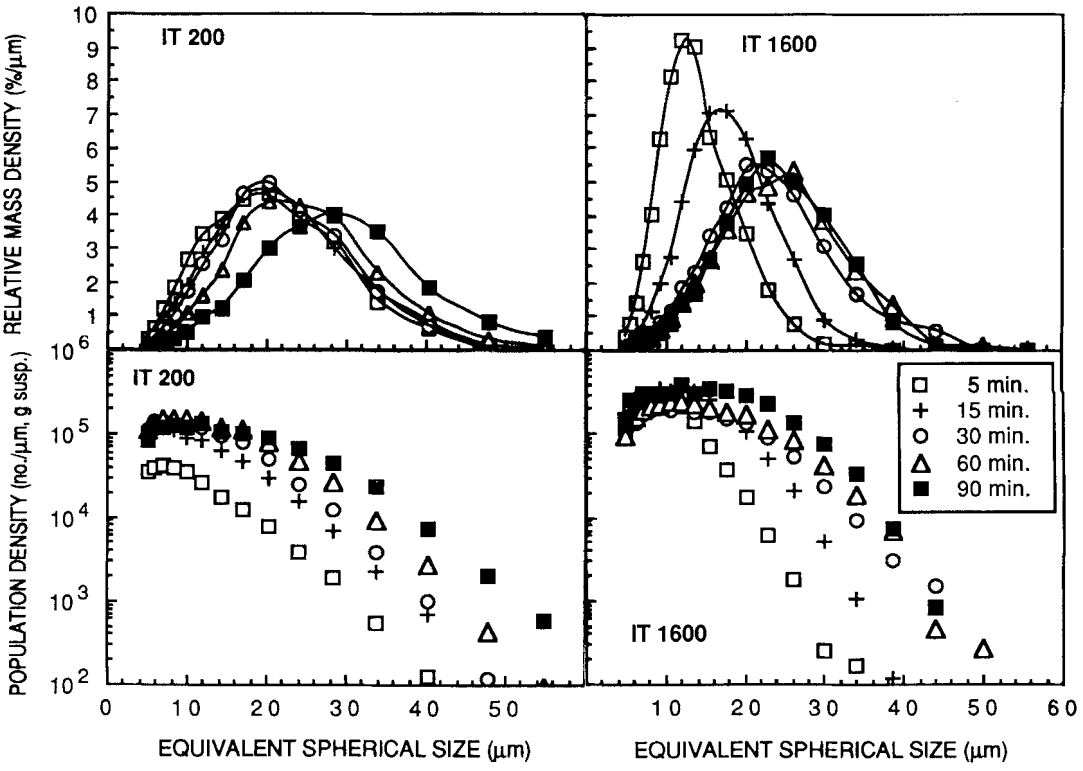

Figure 16. Evolution of size distributions for IT 200 and 1600.

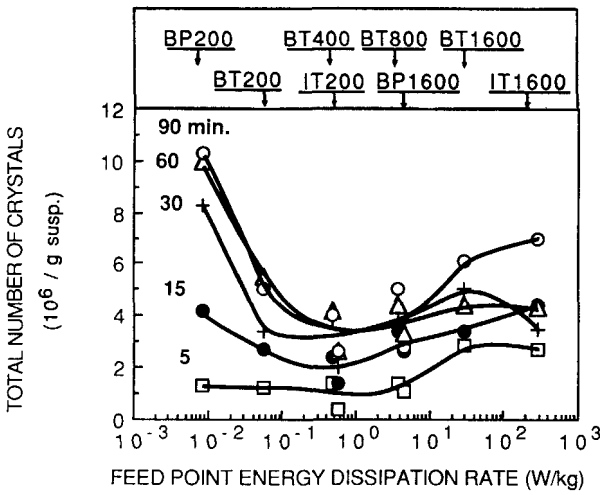

Figure 17. Total numbers of crystals as function of feed point energy dissipation rate.

directly explain the dependence on the feed point as observed in the experimental results. Growth of small crystals is not likely to show a strong dependence on stirring rate for two reasons. At decreasing size, the relative influence of volume diffusion tends to decrease, since the volume diffusion resistance decreases with decreasing size while the surface integration resistance normally is assumed to increase (Jancic and Grootsholten, 1984). Accordingly, often surface integration control has been reported for sparingly soluble salts (Konak, 1974). However, even in the case of volume diffusion control, the influence of stirring rate would decrease with decreasing size as discussed by Nielsen (1969, 1979) and recently thoroughly analyzed by Armenant and Kirwan (1989). At decreasing particle size, the relative velocity to the fluid decreases and the Sherwood number approaches the value of 2. Thus, we conclude that the observed influence of hydrodynamic parameters cannot be explained by a direct influence on the volume diffusion resistance of the crystal growth. The decrease in size at high mixing intensities is to some extent due to abrasion and secondary nucleation. However, as discussed above, some results indicate that the interaction between the feed zone and the bulk volume needs to be analyzed.

Nucleation

In the majority of experiments, 1.4-M HCl is mixed into 0.35-M sodium benzoate (=reactants of medium initial concentration). If 1 volume of acid is mixed with 4 volumes of benzoate, the maximum supersaturation ratio (S_0) becomes approximately 10 when we account for a reduction in solubility due to the sodium chloride concentration (Larsson, 1930). The total range of S_0 in the entire program is from 4 to 28. Accordingly, extensive primary nucleation may take place. Classical treatment of homogeneous nucleation (Nielsen, 1964; Mullin, 1972; Mohanty et al., 1990) results in:

$$J = A \exp\left(-\frac{\Delta G^*}{kT}\right) \tag{1}$$

$$\Delta G^* = \frac{\beta \sigma^3 v_m^2}{(kT \ln S)^2} \tag{2}$$

For heterogeneous nucleation, only empirical relationships exist but the dependence on supersaturation is normally very strong. A time constant for the homogeneous nucleation may be defined as being inversely proportional to the rate of nucleation, J. Accordingly, the so-called induction time depends strongly on the supersaturation ratio, S, and on the value of the interfacial energy, σ. Interfacial energies range from 0.001 to 0.15 J/m^2, and values for several inorganic substances are tabulated by Nielsen and Söhnel (1971) and by Nyvlt et al. (1985). However, no specific value for benzoic acid has been found in the literature. We have performed some experiments of the classic type (Nyvlt et al., 1985) involving instantaneous mixing of reactant volumes in a beaker to estimate induction times. Over a supersaturation ratio from 1.8 to 3.8, the induction time varies from 30 s to 0.6 s, after subtracting 2 s for mixing. When plotted as log t_{ind} vs. (log S_0)$^{-2}$, the data reveal a rather moderate slope.

We have also performed some T-mixer experiments (Nielsen, 1969; Roughton, 1953), in which two reactant streams are mixed, and the distance of the occurrence of turbidity from the point of mixing becomes a measure of the induction time. At $S_0 = 5.2$, we obtain a value of order 0.02 s, and at 6.5 roughly an order of magnitude lower. Equimolar solutions were mixed at turbulent flow, and the linear flow rates were of the order meters/second. The data plotted as described above indicate a still steeper slope. Often transitions are observed (Nielsen, 1969) in data and are interpreted as homogeneous nucleation at the highest supersaturation ratios, heterogeneous nucleation at lower supersaturation, and occasionally a transition in growth mechanism at further reduced supersaturation. From the steepest slope, we may estimate an interfacial energy value of the order 40 mJ/m^2, which corresponds with the generalized plot of Nielsen and Söhnel (1971). Induction times are not well-defined theoretically and when they are in the order of milliseconds, it is difficult to determine them experimentally. However, our results show that for benzoic acid, the range of S, where t_{ind} starts to decrease from a fraction of a second very steeply with (log S)$^{-2}$, coincides rather well with the range of the semibatch experiments. This range differs significantly for different substances. The results suggest that for benzoic acid homogeneous nucleation dominates at $S_0 = 10$ with an induction time in the order of less than milliseconds, and maybe a transition to heterogeneous nucleation occurs around $S_0 = 4$ at an induction time in the order of 0.1 s. If homogeneous nucleation dominates the influence of the air entrainment, at high agitation it should be limited.

Micromixing

A general understanding of mixing (Ulbrecht and Patterson, 1985) and the work of Nielsen (1964) lead us to suggest the following description of this process. In the feed zone, the feed stream is strained into a thin film by the local bulk stream, and it is chopped into a size distribution (in terms of length, width and thickness) of film segments that become wrapped in swirls and are further sheared and strained. The chemical acid-base reaction is considered to be much faster than other rate processes in this system including the micromixing rate, and the formation of benzoic acid accordingly takes place under conditions of partial segregation. On the molecular scale, mixing takes place as a result of molecular diffusion between a layer of feed solution (hydrochloric acid) and a layer of bulk

solution (sodium benzoate). The maximum local supersaturation is determined by the concentrations of the reactant solutions, and the maximum generation rate of benzoic acid occurs at the first contact of layers. Close to the area of contact between layers a region develops (in the following called reaction zone) containing benzoic acid, in which nucleation, if fast enough, and nuclei growth may take place. The longer the contact, the thicker the reaction zone, and since it is controlled by diffusion of reactants, the slower the rate of benzoic acid generation becomes. The nucleation rate would decrease in favor of the growth of nuclei already present. The process is semibatch, and all acid will be consumed sooner or later regardless of mixing intensity; however, if the induction time for nucleation is short, the overall number of nuclei formed should increase with the rate of layer contact area generation and with increasing reaction zone supersaturation, that is, concentrations of reactant solutions. The feed zone region is not necessarily an actual physical spot in the vessel, but the sum of hydrochloric acid-sodium benzoate contact volumes, that is, the acid film segments and the surrounding benzoate solution.

To estimate the time constant for micromixing (small-scale disruption of the feed flow, viscous shearing, and straining and ultimate molecular diffusion), we have to estimate the scale of segregation over which diffusion has to carry out the ultimate mixing. The bulk fluid flow is turbulent. Angst et al. (1982) considered the size of the reaction zone to be equal to the Kolmogoroff microscale of the turbulence in the tank:

$$\lambda_K = \left(\frac{\nu^3}{\epsilon}\right)^{1/4} \tag{3}$$

which decreases with increasing stirring rate to power 3/4. Using the local energy dissipation rates estimated above, the Kolmogoroff microscale for turbine stirring may be calculated to range from 36 μm to 8 μm over the range 200 RPM to 1,600 RPM at a position close to the turbine, and in the bulk the range is 64 μm to 13 μm. However, the feed flow also may influence the feed zone scale of segregation. In all experiments, the feed flow is laminar in the tube and is low compared to the bulk flow caused by agitation. At the feed pipe exit, the flow has the same dimension as the pipe diameter, but it becomes rapidly strained into reduced dimensions when adapting the velocity of the bulk stream. The feed flow scale of segregation will depend on the arrangement of the outlet in relation to the bulk stream. At the position close to the stirrer, it will increase proportional to the feed flow rate and inverse to the stirring rate. Estimating the fluid velocity from the impeller region at 200 RPM gives a value in the order of 0.3 m/s. The corresponding velocity in the bulk position would be about five times lower. When feeding close to the turbine, the ratio of the feed flow scale of segregation to the bulk flow Kolmogoroff microscale is in the order of unity to 0.1. The ratio decreases with increasing stirring rate and with decreasing feed rate. In the bulk feed position, the ratio is about an order of magnitude higher than close to the stirrer, partly because of the cocurrent arrangement. Thus, the influence of the feed flow do not entirely overrule the assumption that the feed zone scale of segregation corresponds to the local Kolmogoroff microscale of turbulence in the tank.

The time to penetrate a slab by molecular diffusion to change the concentration at the center to half its final amount may be estimated by:

$$t_D = 0.38\,\frac{\delta^2}{4D} \tag{4}$$

where δ is the slab thickness. Angst et al. (1982) developed a model in which reaction zone slabs are allowed to be stretched and strained. In a turbulent fluid, the time t_S for laminar shearing of a slab of initial thickness δ_0 to thickness δ may be estimated by:

$$\left(\frac{\delta_0}{\delta}\right)^2 = 1 + 0.25\,\frac{\epsilon}{\nu}\,t_s^2 \tag{5}$$

In comparison to molecular diffusion, the stretching is fast and accordingly of great importance to estimating the micromixing times. In a simplified approach, we may assume stretching to precede molecular diffusion. Allow the same time for stretching from δ_0 to δ as for molecular diffusion in a slab of thickness δ, that is, insert t_D of Eq. 4 for t_S in Eq. 5. Solve for δ, insert into Eq. 4, and multiply the time by 2. Assume that the initial slab thickness equals the Kolmogoroff microscale and insert Eq. 3 for δ_0. If $(\delta_0/\delta)^2 \gg 1$, we may derive at a total micromixing time of:

$$t_{\text{micro}} = 1.45\ \text{Sc}^{1/3}\left(\frac{\nu}{\epsilon}\right)^{1/2} \tag{6}$$

one-half of t_{micro} is the time to shear δ_0 to δ according to Eq. 5, and the other half the time to penetrate a slab of thickness δ by molecular diffusion according to Eq. 4. The assumption $(\delta_0/\delta)^2 \gg 1$ is valid, when straining is given the time to proceed to a significant extent. This is the case when *Sc* is high as for normal water solutions. The mixing time increases with initial slab thickness raised to 2/3 at constant energy dissipation and decreases with energy dissipation to order 1/3, at constant initial slab thickness.

The rate of local energy dissipation in the experiments ranges from about 0.01 W/kg to 250 W/kg, and over this range the micromixing time according to Eq. 6 ranges from 0.15 s to a millisecond. It has been suggested (Baldyga and Bourne, 1984) that the initial size of the reaction zone might be in the order of ten times larger than λ_K. If that is the case, the micromixing times would increase by a factor $10^{2/3}$. The mixing times calculated compares well with the values discussed by Brodkey (1985): 0.02 s close to the impeller and about 0.2 s away from the impeller. The mixing times estimated relate to the intensity of segregation in a relative sense. The absolute concentration levels determine reaction rates, and crystallization. The mixing time to deplete concentration variations to a certain absolute level would increase with reactant concentrations. In Eq. 6 the mixing time decreases with energy dissipation raised to 1/2, as compared to the range 1/3 to 1/2 given by Brodkey (1985). An increase in the stirring rate from 200 RPM decreases the mixing time to 1/8 for 800 RPM and to 1/23 for 1,600 RPM. A ten fold increase of the local energy dissipation rate reduces the mixing time to 1/3.

A more efficient micromixing at the feed point increases the generation rate of reaction zone contact area, which increases the overall consumption rate of hydrochloric acid and gen-

eration rate of benzoic acid. However, the scale of segregation in the feed zone volume is reduced, and as a secondary effect micromixing may proceed and dilute the supersaturation by further mixing into bulk solution. The significance of the latter step depends on whether nucleation is fast and may take place before significant dilution occurs. If the induction time for nucleus formation is shorter than the micromixing time, nuclei may appear and grow in the reaction zone. An increased mixing then increases the rate of nucleation and the product mean size decreases. If the induction time is comparable to or longer than the micromixing time, benzoic acid has the time to be at least partly diluted through micromixing into benzoate solution, thus reducing the supersaturation. Then, increased micromixing will reduce nucleation and favor larger product crystals. The dilution influence on nucleation may either be discussed in terms of the nucleation rate being a very strong function of supersaturation or in terms of total volume of feed zone elements containing labile solution that survives (from being diluted) for a time longer than the induction time for nucleation.

Macromixing and Ostwald ripening

The estimations of induction times and micromixing indicate that at $S_0 = 10$ nucleation is likely to be faster or significantly faster than micromixing. If nuclei have the time to form, they will grow somewhat in the high supersaturation of the reaction zone. Mass is furnished by diffusion of hydrogen ions and benzoate ions, forming benzoic acid, and the growth process proceeds under conditions of partial segregation. The benzoic acid formed may be diluted through further micromixing, including ordinary diffusion. Micromixing dilution may also include a reduction of the amount of hydrogen ions locally available for generation of benzoic acid. Both effects may influence on the growth rate and may also impose a mass constraint on growth in the reaction zone. In the following discussion of nuclei growth we do not distinguish between different aspects of the micromixing dilution of the reaction zone environment. In the bulk solution environment, Ostwald ripening may dissolve tiny crystals if they have not reached a corresponding critical size. Accordingly, mixing may act to interrupt the initial growth process and thus reduce the number of crystals that are stable in the bulk solution. By the Kelvin equation (Mullin, 1972):

$$\frac{c^*(r)}{c_s} = \exp\left(\frac{2\sigma M}{RT\rho_c r}\right) = \exp\left(\frac{K}{r}\right) \tag{7}$$

we may estimate the critical size to approximately 0.0013 μm at $S = 10$, 0.03 μm at $S = 1.1$, and 0.3 μm at $S = 1.01$. The rate of crystal dissolution may be estimated by considering the case of mass transfer from a sphere of subcritical size, r, in a stagnant infinite medium:

$$-\frac{dr}{dt} = \frac{DMc_s}{r\rho_c}\left[\frac{c^*(r)}{c_s} - \frac{c}{c_s}\right] \tag{8}$$

where $c^*(r)$ is obtained from Eq. 7, and c/c_s is the supersaturation ratio in the bulk. K is approximately 3.7×10^{-9} m, and the exponential term deviates significantly from unity, only when r is reasonably close to or smaller than K. Estimations reveal that except for sizes close to the bulk critical size the rate of Ostwald ripening becomes very high for crystals of subcritical sizes. Newly-born crystals may very well dissolve within a range of a fraction of a millisecond to 0.1 s, depending on the size and bulk supersaturation. Using Eq. 8, we may also estimate a maximum (only diffusion-controlled) rate of growth in the feed zone environment by inserting the feed zone concentration for c. For this case, small particles may very well grow into stable sizes within a millisecond, if not limited by mass constraint. However, the crystals are very small, and the supersaturation ratio is moderate. Thus, surface integration resistance may reduce the growth rate and micromixing dilution may prevent growth into stable sizes. In conclusion, nucleation in itself may become reduced by dilution of generated supersaturation, or the initial growth may become reduced, resulting in a more effective ripening. At $S_0 = 4$, the first effect is likely to be important, while at $S_0 = 10$ the second effect seems to dominate. Both mechanisms result in a reduced number of crystals in the bulk to share the final total mass.

Considering the batch as a whole, there is a depletion in benzoate concentration as well as an increase in the content of particles, that is, crystal surface area. From the feed zone to the bulk supersaturation is conveyed, and a size distribution ranging from subcritical sizes, of small crystals. Supersaturation transferred directly or generated by fast ripening allows crystals to grow in the bulk. However, if the supersaturation in the bulk increases, the feed solution becomes mixed and diluted with suspension having already some supersaturation, and the dilution reduction of the effective feed zone nucleation becomes weaker. At high agitation rates, the supersaturation may be particularly high in the bulk early in the process as a result of high reactant concentrations and low total crystal surface area, and we may even envisage something like an effective bulk nucleation. The time for the macroscopic circulation of liquid back to the feed zone is inversely proportional to the stirring rate and is estimated to range from 0.1 to 1 second over the range of turbine stirring in the experiments (Bourne, 1985). Subcritical crystals, recirculated back to the feed zone, have the opportunity to grow into stable sizes, which means that only very fast ripening has the potential of reducing effective nucleation. An increased agitation reduces the circulation time and may result in an increased bulk supersaturation and may thus reverse the influence of mixing on the product particle size.

Interpretation of experimental results

From the analysis above, we conclude that at least four main aspects have to be considered:

1. Increased reaction zone supersaturation, that is, concentration of reactant solutions, increases reaction zone nucleation, if the induction time is short.
2. Increased rate of contact area generation between reactant solutions, that is, reaction zone contact area, increases total feed zone nucleation, if the induction time is short.
3. Increased feed point micromixing and otherwise decreased scale of segregation increase the micromixing dilution rate of the reaction zone environment, which may reduce nucleation or nuclei growth.
4. Increased bulk supersaturation decreases the effect of feed zone dilution and decreases bulk Ostwald ripening.

Based on this, we may suggest the following explanations

to the experimental results. The small product size produced at BP 200 is the result of extensive nucleation at the feed point. The nuclei have the time to form in the feed zone and to grow into stable sizes. Effective nucleation decreases during the process due to decreasing bulk reactant concentration and increasing crystal surface area in the bulk suspension being mixed with feed solution. Both aspects reduce the reaction zone supersaturation.

At IT 200, the micromixing dilution of the reaction zone environment is more efficient. This results in reduced nuclei growth and more dominating Ostwald ripening in the bulk. Accordingly, the effective nucleation becomes lower. At IT 400, these effects are even more pronounced. At further increased feed point mixing, the bulk supersaturation becomes high enough to counteract the feed zone dilution effect. Nuclei growth is not efficiently reduced, and the bulk critical size becomes lower. At IT 1600, the bulk nucleation early in the process increase to a level where a magnified effective nucleation takes place and some similarities with a batch cooling crystallization forced into the labile region may be envisaged. Also breakage, fragmentation, and secondary nucleation become important.

Increasing the feed time decreases the scale of segregation in the feed zone. Micromixing dilution becomes more competitive, and effective nucleation is reduced. Supersaturation increase in the bulk becomes slower. However, as shown in Figure 7, reactant concentrations may be important still at long feeding times. The early moment of contact between fresh reactant solutions will loose the influence only at long induction times, that is, when no nucleation has the time to take place before complete dilution, or at complete Ostwald ripening, that is, no crystals survive in the bulk regardless of feed zone growth. In both cases, the process acts as a well-mixed system. Increasing the hydrochloric acid concentration increases the supersaturation level in the reaction zone, thus increasing nucleation and the mass locally available for growth becomes higher. Controlled feed rate curves are not effective as controlled cooling rates are in cooling crystallization. The controlled feed rate principal fails because local conditions at the feed point are important and the overall rate of supersaturation generation is very high.

The solubility of benzoic acid in 0.35-M sodium benzoate solution is only slightly higher than in 0.35-M hydrochloric acid, and the maximum dissociation we may expect at our conditions is only 5% (Larsson, 1930). We propose that the results of Figure 10 are explained by differences in ionic mobilities and in local solubility conditions. The mobility of the hydrogen ion is five to seven times higher than that of the chloride and sodium ions and 11 times that of the benzoate ion (Reid and Sherwood, 1966). Thus, diffusion of hydrogen ions toward benzoate solution may be faster than the reverse, when electroneutrality is maintained by diffusion of chloride and sodium ions. The feed solution in our experiments always has a higher concentration than the bulk solution, and the maximum benzoic acid concentration locally is determined by the limiting reactant. When feeding hydrochloric acid, the reaction zone allocates more into the bulk solution, since hydrogen diffuses faster toward the surrounding benzoate solution than the reverse, and the maximum benzoic acid concentration tends to be limited by the bulk benzoate concentration (0.35 M). In the reversed situation, higher concentrations may result. For the same reason, the local solubility in the reaction zone may be lower when benzoate is fed to hydrochloric acid instead of the reverse, because the reaction zone sodium chloride concentration may be higher. The concentration and solubility effects cooperate and suggest that the local reaction zone supersaturation is higher when benzoate is fed to hydrochloric acid, thus explaining the reduced product size.

The experimental results of this study contradicts the results of Tosun (1988) concerning the influence of the stirring rate. Tosun (1988) studied crystallization of barium sulfate by feeding sodium sulfate into a stirred solution of barium chloride. A minimum in the product particle size vs. the stirring rate was found. Due to lower solubility, the maximum supersaturation ratio in the experiments of Tosun (1988) is approximately 1,900; however, the estimated corresponding induction time still is approximately 0.02 s (Nielsen, 1961). The range of mean specific power input seems to have been approximately the same as in the present study. However, the reactant feed flow rates used by Tosun are about 15 times higher, and the feed flow linear velocity is about 30 times higher than that in our work. The feed flow scale of segregation becomes significantly larger than the Kolmogoroff microscale of the turbulence in the tank, resulting in increased micromixing times. However, it seems that in relation to induction times the range of mixing times of Tosun are somewhat lower. The use of Eqs. 7 and 8 reveals that the Ostwald ripening rate in the bulk tends to be considerably lower due to the significantly lower solubility of barium sulfate. Concerning the growth rate, Nielsen (1969) suggests that in this case volume diffusion actually is controlling. In the case of volume diffusion-controlled growth in the feed zone, due to the lower solubility in Eq. 8, is significantly counteracted by the high supersaturation ratio, and the feed zone growth rate of barium sulfate may be comparatively high. The observed reduction in mean size at increased mixing may have been caused by the fact that more nuclei are generated in the feed zone due to improved contact, and that either they grow quickly into stable sizes or the ripening in the bulk is too slow to be effective. At higher stirring rates, an increased product size with increased agitation may be explained by the result that dilution reduces either nucleation or the initial growth.

In stoichiometric batch and T-mixer experiments, increased mixing may only increase the rate of reaction zone contact area generation and thus nucleation, since essentially no dilution effect is possible. Accordingly, these experiments normally reveal a decreased size at increased mixing.

The discussion exposes the complexity of a semibatch reaction crystallization and at present we are only able to indicate possible explanations to the experimental results. There is a strong need for fundamental work in this area, before these processes are fully understood. In particular the conditions in the reaction zone, where the chemical reaction, crystal nucleation and nuclei growth proceed under conditions of partial segregation, need to be analysed in detail. The feed flow is strained into a very thin film, the thickness of which, at low feed rates and high agitation, approaches the dimension of nuclei that are stable in the bulk. Thus, the mass locally available for nuclei growth into stable sizes may be insufficient. A detailed analysis should clearly distinguish between the scale of segregation of the turbulence in the tank, and the dimensions

of the strained feed stream. A valuable contribution concerning the fundamentals of reaction crystallization has recently been published by Wachi and Jones (1991).

Conclusions

Process variables may influence significantly the product crystal size distribution in the semibatch reaction crystallization of a low-soluble substance. The stirring rate, feed point position, feed rate, and reactant concentrations affect the weight mean size of benzoic acid, which varies from 17 μm to 55 μm. In general, increased feed point mixing intensity and reduced feed point reactant concentrations favor the production of larger crystals. At high mixing intensities, the weight mean size decreases with increased agitation.

The product of a semibatch reaction crystallizer is the result of complex interactions of several phenomena. The rates of nucleation and nuclei growth have to be compared with the rate of feed point micromixing. The chemical reaction, crystal nucleation and nuclei growth may proceed under conditions of partial segregation, in which case the analysis has to consider the molecular level conditions of the reaction zone. Feed point micromixing brings reactants together and reactant concentrations determine the maximum supersaturation and thus the nucleation, that may occur in the reaction zone. Micromixing may also continue and dilute the local environment in which nucleation and nuclei growth take place. Tiny crystals conveyed into the bulk solution may dissolve as a result of Ostwald ripening, depending on the bulk supersaturation. The bulk supersaturation, in turn, is dependent on the rate of conveyance of supersaturation from the feed zone, on the rate of generation as a result of Ostwald ripening and on the rate of consumption due to growth. The properties of the bulk suspension influence on the generation and consumption of supersaturation in the feed zone as well as on the micromixing dilution. The discussion of experimental results is based on these different aspects and explanations are suggested. In the present study the reactant concentrations in most of the experiments are high enough to result in nucleation at the instant of reactant contact. The product crystal size increases with increased feed point mixing intensity as a result of increased micromixing dilution of the nuclei growth environment. Smaller crystals are conveyed to the bulk and Ostwald ripening becomes more efficient. At low reactant concentrations, the induction time becomes comparable to the micromixing time and dilution may hamper nucleation itself. At high feed point mixing, the bulk supersaturation rises which in turn reduces the efficiency of the dilution and of the Ostwald ripening. A magnified effective nucleation may take place and result in a reduced product size.

Acknowledgment

The financial support of The Swedish Board for Technical Development (STU), the Swedish Council for Planning and Coordination of Research (FRN), and the Swedish Industrial Association for Crystallization Research and Development (IKF) is gratefully acknowledged.

Notation

A = parameter in Eq. 1, m
c = concentration, kmol·m^{-3}
$c^*(r)$ = solubility of crystal of size r, kmol·m^{-3}
c_s = solubility of large particles ($r \to \infty$), kmol·m^{-3}
D = diffusivity, m^2·s^{-1}
ΔG^* = change in Gibbs free energy (formation of nuclei of critical size), J
J = rate of nucleation, m^{-3}·s^{-1}
K = parameter in Eq. 7, m
L_i = crystal mean size of size interval, m
L_{43} = crystal weight mean size, m
M = molecular weight, kg·kmol^{-1}
N_i = number of particles in size interval
r = particle radius, m
R = gas constant, 8.317 J·mol^{-1}·K^{-1}
S = c/c_s, supersaturation ratio
S_0 = initial supersaturation ratio
Sc = ν/D, Schmidt's number
SD = width of size distribution, m
t = time, s
T = temperature, K
t_D = half-life time for molecular diffusion, s
t_{ind} = induction time, s
t_{micro} = micromixing time, s
t_s = time for laminar shearing of a slab, s
v_m = molecular volume, m^3

Greek letters

β = dimensionless geometric shape factor
δ = slab thickness, m
δ_0 = initial slab thickness, m
ϵ = energy dissipation rate, W·kg^{-1}
λ_k = Kolmogoroff turbulence microscale, m
ρ_c = crystal density, kg·m^{-3}
ν = kinematic viscosity, m^2·s^{-1}
σ = interfacial tension, J·m^{-2}

Literature Cited

Angst, W., J. R. Bourne, and R. N. Sharma, "Mixing and Fast Chemical Reaction: IV. The Dimensions of the Reaction Zone," *Chem. Eng. Sci.*, **37**(4), 585 (1982).

Armenante, P. M., and D. J. Kirwan, "Mass Transfer to Microparticles in Agitated Systems," *Chem. Eng. Sci.*, **44**(12), 2781 (1989).

Baldyga, J., and J. R. Bourne, "Initial Deformation of Material Elements in Isotropic, Homogeneous Turbulence," *Chem. Eng. Sci.*, **39**(2), 329 (1984).

Bourne, J. R., *Mixing in the Process Industries*, Chap. 10, N. Harnby, M. F. Edwards, and A. W. Nienow, eds., Butterworths (1985).

Brodkey, R. S., "Fundamentals of Turbulent Mixing and Kinetics in Mixing of Liquids by Mechanical Agitation," J. J. Ulbrecht and G. K. Patterson, eds., Gordon and Breach Science Publishers, London (1985).

Fitchett, D. E., and J. M. Tarbell, "Effect of Mixing on the Precipitation of Barium Sulfate in an MSMPR Reactor," *AIChE J.*, **36**(4), 511 (1990).

Franck, R., R. David, J. Villermaux, and J. P. Klein, "Crystallization and Precipitation Engineering: II. a Chemical Engineering Approach to Salicylic Acid Precipitation: Modeling of Batch Kinetics and Application to Continuous Operation," *Chem. Eng. Sci.*, **43**(1), 69 (1988).

Gunn, D. J., and M. S. Murthy, "Kinetics and Mechanisms of Precipitations," *Chem. Eng. Sci.*, **27**(6), 1293 (1972).

Gutoff, E. B., F. R. Cottrell and E. G. Denk, "Scale-Up Factors in the Batch Precipitation of Silver Halide Photographic Emulsions," *Photographic Sci. and Eng.*, **22**(6), 325 (1978).

O'Hern, H. A., and F. E. Rush, Jr., "Effect of Mixing Conditions in Barium Sulphate Precipitation," *Ind. Eng. Chem. Fundam.*, **2**(4), 267 (1963).

Jancic, S. J., and P. A. M. Grootsholten, *Industrial Crystallization*, Delft University Press, D. Reidel Co., Dordrecht (1984).

Kirk-Othmer, D. F., *Encyclopedia of Chemical Technology*, 3rd ed., Vol. 7, Interscience Publ., New York (1979).

Konak, A. R., "A New Model for Surface Reaction-Controlled Growth of Crystals from Solution," *Chem. Eng. Sci.*, **29**, 1537 (1974).

Kuboi, R., M. Haranda, J. M. Winterbottom, A. J. S. Anderson, and A. W. Nienow, "Mixing Effects in Double-Jet and Single-Jet Precipitation," World Congress of Chemical Engineering, Part II, Tokyo, 8g-302 (1986).

Larsson, E., "Die Löslichkeit von Säuren und Salzlösungen: II. Die Löslichkeit der Benzoesäure und der Aktivitetskoeffizient ihrer Moleküle in wässerigen Benzoatlösungen," *Zeitschrift für Physikalische Chemie*, **148 A**, 148 (1930).

Larsson, E., "Die Löslichkeit von Säuren und Salzlösungen: III. Die Löslichkeit der Benzoesäure und der Aktivitetskoeffizient ihrer Moleküle in Lösung von Natriumchlorid und Kaliumchlorid," *Zeitschrift für Physikalische Chemie*, **148A**, 304 (1930).

Mohanty, R., S. Bhandarkar, B. Zuromski, R. Brown, and J. Estrin, "Characterizing the Product Crystals from a Mixing Tee Process," *AIChE J.*, **34**(12), 2063 (1988).

Mullin, J. W., *Crystallisation*, Butterworths, London (1972).

Mullin, J. W., and M. M. Osman, "Characteristics of Nickel Ammomium Sulphate Crystals Precipitated from Aqueous Solution," *Kristall und Tecknik*, **8**(7), 779 (1973).

Mullin, J. W., S. Zacek, and J. Nyvlt, "Batch Precipitation of Potash Alum Crystals by Mixing Aqueous Solutions of the Component Salt," *Crystal Res. & Technol.*, **17**(5), 617 (1982).

Nielsen, A. E., "Homogeneous Nucleation in Barium Sulphate Precipitation," *Acta. Chem. Scand.*, **15**(2), 441 (1961).

Nielsen, A. E., *Kinetics of Precipitation*, University of Copenhagen, Pergamon Press, Oxford (1964).

Nielsen, A. E., "Nucleation and Growth of Crystals at High Supersaturation," *Kristall und Technik*, **4**(1), 17 (1969).

Nielsen, A. E., and O. Söhnel, "Interfacial Tensions Electrolyte Crystal-Aqueous Solution, from Nucleation Data," *J. of Crystal Growth*, **11**, 233 (1971).

Nielsen, A. E., "Kinetics of Crystal Growth during Precipitation of a Binary Electrolyte," *Symp. on Industrial Crystallization*, E. J. de Jong and S. J. Jancic, eds., North Holland Publishing, 159 (1979).

Nyvlt, J., O. Söhnel, M. Matuchova, and M. Broul, "The Kinetics of Industrial Crystallization," *Chemical Engineering Monographs 19*, Elsevier, Amsterdam (1985).

Okamoto, Y., M. Nishikawa, and K. Hashimoto, "Energy Dissipation Rate Distribution in Mixing Vessels and its Effects on Liquid-Liquid Dispersion and Solid-Liquid Mass Transfer," *Int. Chem. Eng.*, **21**(1), 88 (1981).

Oldshue, J. Y., *Fluid Mixing Technology*, McGraw-Hill, New York (1983).

Pohorecki, R., and J. Baldyga, "The Use of a New Model of Micromixing for Determination of Crystal Size in Precipitation," *Chem. Eng. Sci.*, **38**(1), 79 (1983).

Pohorecki, R., and J. Baldyga, "The Effect of Micromixing on the Course of Precipitation in an Unpremixed Feed Continuous Tank Crystallizer," Euro. Conf. on Mixing, Wurzburg, BHRA, Paper 12 (1985).

Ramsden, J. J., "Nucleation and Growth of Small CdS Aggregates by Chemical Reaction," *Surface Sci.*, **156**, 1027 (1985).

Reid, R. C., and T. K. Sherwood, *The Properties of Gases and Liquids*, 2nd ed., McGraw-Hill, New York (1966).

Roughton, F. J. W., *Technique of Organic Chemistry*, Vol. VIII, Part 1, A. Weissberger, ed., Interscience Publishers, New York (1953).

Rousseau, R. W., K. K. Li, and W. L. McCabe, "The Influence of Seed Crystals Size on Nucleation Rates," *AIChE Symp. Ser.*, **72**(153), 48 (1976).

Stavek, J., I. Fort, J. Nyvlt, and M. Sipek, "Influence of Hydrodynamic Conditions on the Controlled Double-Jet Precipitation of Silver Halides in Mechanically Agitated Systems," Euro. Conf. Mixing, Pravia, BHRA, 171 (1988).

Tavare, N. S., and J. Garside, "Simulation of Reactive Precipitation in a Semi-Batch Crystallizer," *Trans. Inst. Chem. Engrs. A.*, **68**(3), 115 (1990).

Tosun, G., "An Experimental Study of the Effect of Mixing on the Particle Size Distribution in $BaSO_4$ Precipitation Reaction," Euro. Conf. on Mixing, Pravia, BHRA, 161 (1988).

Toyokura, K., K. Tawa, and J. Ueno, "Reaction Crystallization of Sulfamic Acid from Urea and Fuming Sulfuric Acid," *Chem. Eng. of Japan*, **12**(1), 24 (1979).

Ulbrecht, J. J., and G. K. Patterson, *Mixing of Liquids by Mechanical Agitation*, Gordon Breach Sci. Publ. (1985).

Wachi, S., and A. G. Jones, "Mass Transfer with Chemical Reaction and Precipitation," *Chem. Eng. Sci.*, **46**(4), 1027 (1991).

Wey, J. S., J. P. Terwilliger, and A. D. Girgello, "Analysis of AgBr Precipitation in a Continuous Suspension Crystallizer," *AIChE Symp. Ser.*, **76**(193), 34 (1980).

Åslund, B., "Crystal Size Distribution Control in Reaction Crystallization," Licentiate Treatise, Dept. of Chem. Eng., Royal Inst. of Techn., Stockholm, Sweden (1989).

Åslund, B., and Å. C. Rasmuson, "An Applied Study of Batch Reaction Crystallization," Symp. on Industrial Crystallization, J. Nyvlt and S. Zacek, eds., Elsevier, 603 (1989).

Åslund, B., and Å. C. Rasmuson, "Crystal Size Distribution Control in Semi-Batch Reaction Crystallization," Symp. on Industrial Crystallization, A. Mersmann, ed., Garmisch-Partenkirchen, Germany (1990).

Manuscript received Sept. 20, 1989, and revision received July 30, 1991.